Received: 12 April 2022 | Accepted: 6 July 2022

DOI: 10.1002/hep4.2053

ORIGINAL ARTICLE

Reduction in gut-derived MUFAs via intestinal stearoyl-CoA desaturase 1 deletion drives susceptibility to NAFLD and hepatocarcinoma

Simon Ducheix[1] | **Elena Piccinin**[2] | **Claudia Peres**[3] | **Oihane Garcia-Irigoyen**[1] | **Justine Bertrand-Michel**[4,5] | **Allan Fouache**[6,7] | **Marica Cariello**[1] | **Jean-Marc Lobaccaro**[6,7] | **Hervé Guillou**[8] | **Carlo Sabbà**[1] | **James M. Ntambi**[9] | **Antonio Moschetta**[1,3]

[1]Department of Interdisciplinary Medicine, University of Bari "Aldo Moro", Bari, Italy

[2]Department of Basic Medical Science, Neurosciences, and Sense organs, University of Bari "Aldo Moro", Bari, Italy

[3]INBB, National Institute for Biostructures and Biosystems, Rome, Italy

[4]MetaboHUB-MetaToul, National Infrastructure of Metabolomics and Fluxomics, Toulouse, France

[5]I2MC, Université de Toulouse, Inserm, Université Toulouse III–Paul Sabatier, Toulouse, France

[6]INSERM U 1103, CNRS, UMR 6293, Université Clermont Auvergne, GReD, Aubière, France

[7]Centre de Recherche en Nutrition Humaine d'Auvergne, Clermont-Ferrand, France

[8]Integrative Toxicology and Metabolism Team, Toxalim (Research Centre in Food Toxicology), Université de Toulouse, INRA, ENVT, INP-Purpan, UPS, Toulouse, France

[9]Departments of Biochemistry and of Nutritional Sciences, University of Wisconsin Madison, Madison, Wisconsin, USA

Correspondence
Antonio Moschetta, Department of Interdisciplinary Medicine, University of Bari Aldo Moro, 70124 Bari, Italy.
Email: antonio.moschetta@uniba.it

Funding information
Associazione Italiana per la Ricerca sul Cancro; European Commission; Ministero dell'Istruzione, dell'Università e della Ricerca; POR Puglia

Abstract

Nonalcoholic fatty liver disease (NAFLD) is defined by a set of hepatic conditions ranging from steatosis to steatohepatitis (NASH), characterized by inflammation and fibrosis, eventually predisposing to hepatocellular carcinoma (HCC). Together with fatty acids (FAs) originated from adipose lipolysis and hepatic lipogenesis, intestinal-derived FAs are major contributors of steatosis. However, the role of mono-unsaturated FAs (MUFAs) in NAFLD development is still debated. We previously established the intestinal capacity to produce MUFAs, but its consequences in hepatic functions are still unknown. Here, we aimed to determine the role of the intestinal MUFA-synthetizing enzyme stearoyl-CoA desaturase 1 (SCD1) in NAFLD. We used intestinal-specific *Scd1*-KO (i*Scd1*$^{-/-}$) mice and studied hepatic dysfunction in different models of steatosis, NASH, and HCC. Intestinal-specific *Scd1* deletion decreased hepatic MUFA proportion. Compared with controls, i*Scd1*$^{-/-}$ mice displayed increased hepatic triglyceride accumulation and derangement in cholesterol homeostasis when fed a MUFA-deprived diet. Then, on Western diet feeding, i*Scd1*$^{-/-}$ mice triggered inflammation and fibrosis compared with their wild-type littermates. Finally, intestinal-*Scd1* deletion predisposed mice to liver cancer. *Conclusions*: Collectively, these results highlight the major importance of intestinal MUFA metabolism in maintaining hepatic functions and show that gut-derived MUFAs are protective from NASH and HCC.

This is an open access article under the terms of the Creative Commons Attribution-NonCommercial-NoDerivs License, which permits use and distribution in any medium, provided the original work is properly cited, the use is non-commercial and no modifications or adaptations are made.
© 2022 The Authors. *Hepatology Communications* published by Wiley Periodicals LLC on behalf of American Association for the Study of Liver Diseases.

INTRODUCTION

Nonalcoholic fatty liver disease (NAFLD) has reached epidemic proportions worldwide.[1] Widely considered as the hepatic manifestation of metabolic syndrome,[2] NAFLD encompasses several pathologies ranging from benign and reversible simple steatosis to more severe steatohepatitis (NASH), which can further degenerate into cirrhosis and more rarely evolves into hepatocellular carcinoma (HCC). The classical pattern of NAFLD progression is a two-step model: hepatic steatosis is the first stage and sensitizes the liver to second signals triggering inflammation and hepatic damages important for steatohepatitis development. However, new insights in the comprehension of these diseases have led to a re-assessment of NAFLD progression that gave raise to a "multiple parallel hit" model.[3] Because steatosis is a common feature of NAFLD, lipid metabolism has been deeply studied in this pathology, giving particular attention to the hepatic *de novo* lipogenesis and the fatty acid (FA) processing pathways, as these processes furnish about 25% of the hepatic FAs that accumulate in steatotic liver.[4]

Stearoyl-CoA desaturase 1 (SCD1) is a 37-kDa protein anchored in the endoplasmic reticulum, which catalyzes the introduction of a double bound into saturated FAs to produce monounsaturated FAs (MUFAs). More precisely, SCD1 produces oleic and palmitoleic acids from stearic and palmitic acids, respectively. The biological roles of SCD1 have been deciphered by the generation of mice deleted for *Scd1*.[5] SCD1 is a major regulator of energy metabolism: total body *Scd1* knockout mice (SCD1-KO) are lean, hypermetabolic, and protected from diet-induced[5] and genetic-driven[6] obesity, thus suggesting a deleterious role for SCD1 in a context of metabolic diseases. However, SCD1-KO mice, despite an anti-atherogenic metabolic profile, display more atherosclerosis and higher circulating inflammatory markers[7] and are more susceptible to triggers NASH when fed a methionine/choline-deficient diet,[8] emphasizing a potent beneficial role of this enzyme. SCD1 also plays an important role in skin, as SCD1-KO mice present a defect in skin permeability coupled with heat leak.[9] This skin defect explains a large part of the phenotype observed in SCD1-KO mice. Indeed, hepatic-specific *Scd1* deletion does not recapitulate the phenotype displayed by the total body deletion, as liver KO mice are not protected from steatosis induced by a high-fat diet.[10] Thus, we cannot exclude that the MUFAs produced from other organs could be important in NAFLD, especially because this kind of interorgan MUFA communication has been already described in liver and adipose tissue.[11]

The intestine is one of the organs most closely intertwined with the liver, and it is now clearly established that gut defects may lead to NAFLD development (extensively reviewed in Marra and Svegliati-Baroni[12]). Growing evidence shows that dysregulation of sugar metabolism[13,14] and lipid synthesis[15] in the gut affects systemic energy homeostasis, including the liver.[13,14] However, to date, the role of intestinal MUFA production has not been evaluated. We previously generated mice deficient for *Scd1* specifically in the intestinal epithelium, and showed that these mice were more prone to trigger inflammation and cancer in the gut,[16] but we had not explored the hepatic phenotype.

Here, we aimed to study the hepatic consequences of the intestinal *Scd1* deletion. We challenged intestinal *Scd1*-KO (i*Scd1*$^{-/-}$) mice with different models of NAFLD and HCC, and then assessed several markers of hepatic dysfunctions and lipid metabolism. Reduction in gut-derived MUFAs via intestinal *Scd1* deletion deregulated hepatic lipid and cholesterol metabolism and rendered mice susceptible to develop liver inflammation, fibrosis, and cancer.

METHODS

Generation of mouse models and experimental settings

Scd1$^{fl/fl}$ mice have already been described elsewhere,[10] and we previously generated i*Scd1*$^{-/-}$ mice by crossing the *Scd1*$^{fl/fl}$ line with mice expressing the Cre recombinase under the promoter of the villin.[16] Mice fed control (CTRL) or oleic acid–deficient (OAD) diet were sacrificed at 3 months old. OAD feeding ranged from 1 month old to the end of the experiment. Mice fed the chow or cholesterol (2%) enriched chow diet were sacrificed at 3 months old. They were fed the two diets 1 week before their sacrifice. Mice fed chow or Western diets (WD) were sacrificed at 6 months old. WD feeding ranged from 2 months old to the end of the experiment. For the HCC model, 2-week-old pups were intraperitoneally injected with 25 mg/kg of diethylnitrosamine (DEN) and were sacrificed after 1 year. All mice used in the experiments were males with a C57BL/6 background. All mice were sacrificed random fed at ZT 3. Mice were kept in a pathogen-free facility, at 21 ± 2°C with a 12-h light/dark cycle and had free access to food and water.

Dietary regimens

Chow diet (Global diet 2018) was purchased from Teklad. Control diet (CT; D15013003B) and oleic acid deficient diet (OAD; D15013004), purchased from Research Diet, are isocaloric and contain 5% of fat. The percentage of oleic acid is 1% for OAD and 24% for CT. The composition and the FA profile of these diets are provided in Tables S1 and S2, respectively.

The WD (D12079B) contains 21% wt of fat and 0.2% wt of cholesterol and was from Research Diet. The results regarding the chow and Western part are separated in Figure 4 because the "chow" and "Western" parts were conducted separately.

Blood and organ sampling

Blood was collected by cardiac puncture in heparin-coated capillaries. Plasma was prepared by centrifugation (1500 *g*, 10 min) and kept at −80°C until use. Following euthanasia, tissues were removed, dissected (for small intestine sections, the mucosa was scrapped on ice), snap-frozen in liquid nitrogen, and stored at −80°C until use. For tumors count experiments, macroscopic analyzes were performed before freezing the liver.

Gene-expression studies

Total RNA was extracted with a Qiazol reagent. For real-time quantitative polymerase chain reaction (qPCR), total RNA samples (2 μg) were treated with DNAse (Thermo Fisher Scientific) and reverse-transcribed using a High-Capacity cDNA Reverse Transcription Kit (Thermo Fisher Scientific). Primers for SYBR Green assays are presented in Table S3. Amplifications were performed on a QuantStudio5 System (Thermo Fisher Scientific). The quantitative PCR data were normalized (ΔΔCT method) by TATA-box binding protein (*Tbp*) messenger RNA (mRNA) levels.

Histology

Tissue samples were fixed in 4% formalin for 24 h, dehydrated, and paraffin-embedded. Liver sections were stained with hematoxylin and eosin (H&E) following standard protocols. Steatosis score was calculated according to Kleiner et al.[17] For immunohistochemistry, sections were subjected to antigen retrieval by boiling the slides in sodium citrate pH 6 (Sigma Aldrich) for 15 min and then permeabilized in phosphate-buffered saline (PBS) with 0.25% TritonX-100 for 5 min. Subsequently, after 10-min incubation at room temperature in protein-blocking solution (Dako), sections were incubated at 4°C for 24 h with the anti-F4/80 antibody (#70076; Cell Signaling Technology). Sections were washed in PBS for 15 min and incubated for 25 min at room temperature with the Dako real EnVision detection system (Peroxidase/DAB+) according to the manufacturer's instructions. For hepatic fibrosis evaluation, 4-μm-thick sections were stained with Direct Red 80 and Fast Green FCF (Sigma-Aldrich). Image processing was performed using ImageJ (National Institutes of Health) software.

Lipidomic analysis

FAs were extracted from frozen tissues using a modified Bligh and Dyer extraction method. Samples were lysed in a water ethylene glycol tetraacetic acid (5 mm)/methanol mix (1:2 vol/vol). Methanol and dichloromethane were added to reach the following ratios of MeOH/water/CH_2Cl_2: 2.5/2.0/2.5. Glyceryltrinonadecanoate was added as an internal standard. The dried lipid extract was transmethylated with 1 ml of BF3 in methanol (1:20, vol/vol) for 60 min at 100°C, evaporated to dryness, and the fatty acid methyl esters (FAMEs) were extracted with hexane/water (3:1). The organic phase was evaporated to dryness and dissolved in 50 μl ethyl acetate. One microliter of FAME was analyzed by gas-liquid chromatography on a 5890 Hewlett-Packard system using a Famewax fused-silica capillary column (30 m, 0.32 mm i.d., 0.25-mm film thickness; Restek). Oven temperature was programmed from 110ºC to 220°C at a rate of 2°C/min, and the carrier gas was hydrogen (0.5 bar). The injector and the detector were at 225ºC and 245°C, respectively. Neutral lipids were extracted from liver or intestine frozen tissues using a Bligh and Dyer extraction method. The dried lipid extracts were re-suspended in isopropanol, and triglyceride (TG) and cholesterol were measured with a colorimetric kit (Sentinel Diagnostic), according to the manufacturer's instructions.

In vitro liver X receptor activity assay

The capacity of the OAD-fed i*Scd1*$^{+/+}$ and i*Scd1*$^{-/-}$ plasma to modulate liver X receptor (LXR) transcriptional activity *in vitro* using the UAS DBD_{GAL4}-LBD_{LXRa} and UAS DBD_{GAL4}-LBD_{LXRb} systems has been adapted from Fouache et al.[18] Briefly, HeLa cells were seeded on a 96-well plaque at 12,500–15,000 cells per well in Dulbecco's modified Eagle's medium (DMEM) supplemented with 10% fetal calf serum. The day after, cells were transfected (JetPrime, Polyplus transfection). All plasmids were prepared at a final concentration of 100 ng/μl: GAL4-responsive MH100(UAS)x4-tk-LUC reporter together with DBD_{GAL4}-$LBD_{LXR\alpha}$ or DBD_{GAL4}-$LBD_{LXR\beta}$, corresponding to the ligand-binding domain (LBD) of human LXRs inserted into pCMX-GAL4 vector. On day 3, cells were washed with PBS 1 time. DMEM supplemented with 10% of plasma from OAD-fed i*Scd1*$^{+/+}$ or i*Scd1*$^{-/-}$ mice was then added 24 h after induction. Luciferase activity was assayed using a Micro LumatPlus LB96V Microplate Luminometer (Berthold Technologies) and normalized by protein content.

Statistical analysis

Data are presented as mean ± SEM. Differential effects were analyzed by Student's *t* tests or by analysis of variance followed by Student's *t* tests in case of more than two experimental conditions. A p value < 0.05 was considered significant.

RESULTS

Intestinal deletion of *Scd1* affects hepatic FA metabolism

Given the major importance of the gut in systemic energy homeostasis, we wanted to explore whether intestinal *Scd1* deletion would impact extra-intestinal organs. We previously showed that intestinal epithelial deletion of *Scd1* decreases MUFA content in small intestine and colon.[16] As the liver is tightly connected to the gut, notably via the portal and lymphatic circulations, we first explored whether modulation of intestinal endogenously produced MUFAs would affect hepatic FA profile. To do so, we assayed the hepatic FA profile in i*Scd1*$^{+/+}$ and i*Scd1*$^{-/-}$ mice fed a regular diet. Gas chromatography of saponified hepatic lipid extracts revealed a decrease of both oleic (C18:1 n-9) and palmitoleic (C16:1 n-7) acid proportions in i*Scd1*$^{-/-}$ versus i*Scd1*$^{+/+}$ mice (Figure 1A). We also computed the delta 9 desaturase activity and observed a decrease of this parameter in i*Scd1*$^{-/-}$ mice versus their wild-type littermates (Figure 1B). These modulations occurred in the absence of any compensation of hepatic *Scd1* expression, suggesting a direct effect of gut-produced MUFAs on hepatic FA profile (Figure 1C). Moreover, we measured hepatic somatic index, TG, and cholesterol levels in the liver and circulating transaminases levels (alanine aminotransferase [ALT] and aspartate aminotransferase [AST]). Intestinal deletion of *Scd1* does not alter these variables (Figure 1D–G). Thus, in a basal condition, intestinal MUFA synthesis modulates hepatic FA profile without consequences on other NAFLD-linked parameters.

Dietary MUFA deficiency triggers TG and cholesterol accumulation in i*Scd1*$^{-/-}$ mice

In our previous study, we showed that oleic acid contained in regular diet could blunt the consequences of the intestinal *Scd1* deletion.[16] To unveil a potent phenotype linked with NAFLD, we fed i*Scd1*$^{-/-}$ mice and their wild-type littermates an oleate deficient diet (OAD) for 8 weeks. The OAD fat content is almost exclusively made of TGs esterified with saturated FA, and such a diet has been shown to trigger hepatic *de novo* lipogenesis and steatosis.[19] Following OAD diet feeding, intestinal *Scd1* deletion did not affect liver somatic index (Figure 2A) nor triglyceridemia (Figure 2B), but increased cholesterolemia (Figure 2B), hepatic TG (Figure 2C), and cholesterol (Figure 2C) content. To determine whether hepatic TG accumulation would be a consequence of increased lipid absorption, we performed an oral gavage with TGs and observed a nonsignificant trend toward a higher absorption in i*Scd1*$^{-/-}$ versus i*Scd1*$^{+/+}$ mice (Figure 2D). As steatosis can predispose to a more severe phenotype, we measured circulating levels of transaminases (ALT and AST [Figure 2E]) and the expression of several genes related with inflammation (tumor necrosis factor alpha [*Tnfa*] and *F4/80*) and fibrosis (alpha smooth muscle actin [*Asma*] and collagen 1a1 [*Col1a1*]) (Figure 2F). Here, the more marked hepatic TG accumulation in the i*Scd1*$^{-/-}$ mice is not associated with increased transaminases nor markers of inflammation or fibrosis levels.

OAD-induced steatosis in i*Scd1*$^{-/-}$ mice is linked with dysregulation of cholesterol metabolism

Cholesterol is a master mediator of NAFLD and particularly the development of NASH.[20] Moreover, total body *Scd1*-KO mice fed a MUFA-deprived diet display hypercholesterolemia and high hepatic cholesterol levels.[21,22] Saturated FA-rich diets, like the OAD diet, have been shown to affect hepatic cholesterogenesis.[23] Thus, we next wanted to determine the origins of cholesterol metabolism dysregulation in i*Scd1*$^{-/-}$ mice fed the OAD diet. First, we wondered whether hepatic cholesterol accumulation in i*Scd1*$^{-/-}$ mice could result from increased hepatic *de novo* synthesis driven by the sterol regulatory element binding protein 2 (SREBP2) pathway. Therefore, we assayed the expression of *Hmgcr* (3-hydroxy 3-methylglutaryl-CoA reductase), *Fdps* (farnesyl diphosphate synthase) and *Mvd* (mevalonate diphosphate decarboxylase) genes, which are under the control of the SREBP2 transcription factor and encode enzymes of the mevalonate pathway. Intestinal *Scd1* deletion did not raised their expression (Figure 3A). Thus, we assumed that hepatic cholesterol accumulation is not due to an increased *de novo* synthesis. In our previous report,[16] we showed i*Scd1*$^{-/-}$ mice fed the OAD diet display higher intestinal proliferation, a process that requires cholesterol.[24] To determine whether cholesterol metabolism could be disturbed in the intestine, we measured ileal mucosa cholesterol content and observed an increased cholesterol level in i*Scd1*$^{-/-}$ versus wild-type mice (Figure 3B). Such accumulation could result from an increased intestinal cholesterol absorption, which is driven through NPC1 like intracellular cholesterol transporter 1 (NPC1L1) and is facilitated by bile

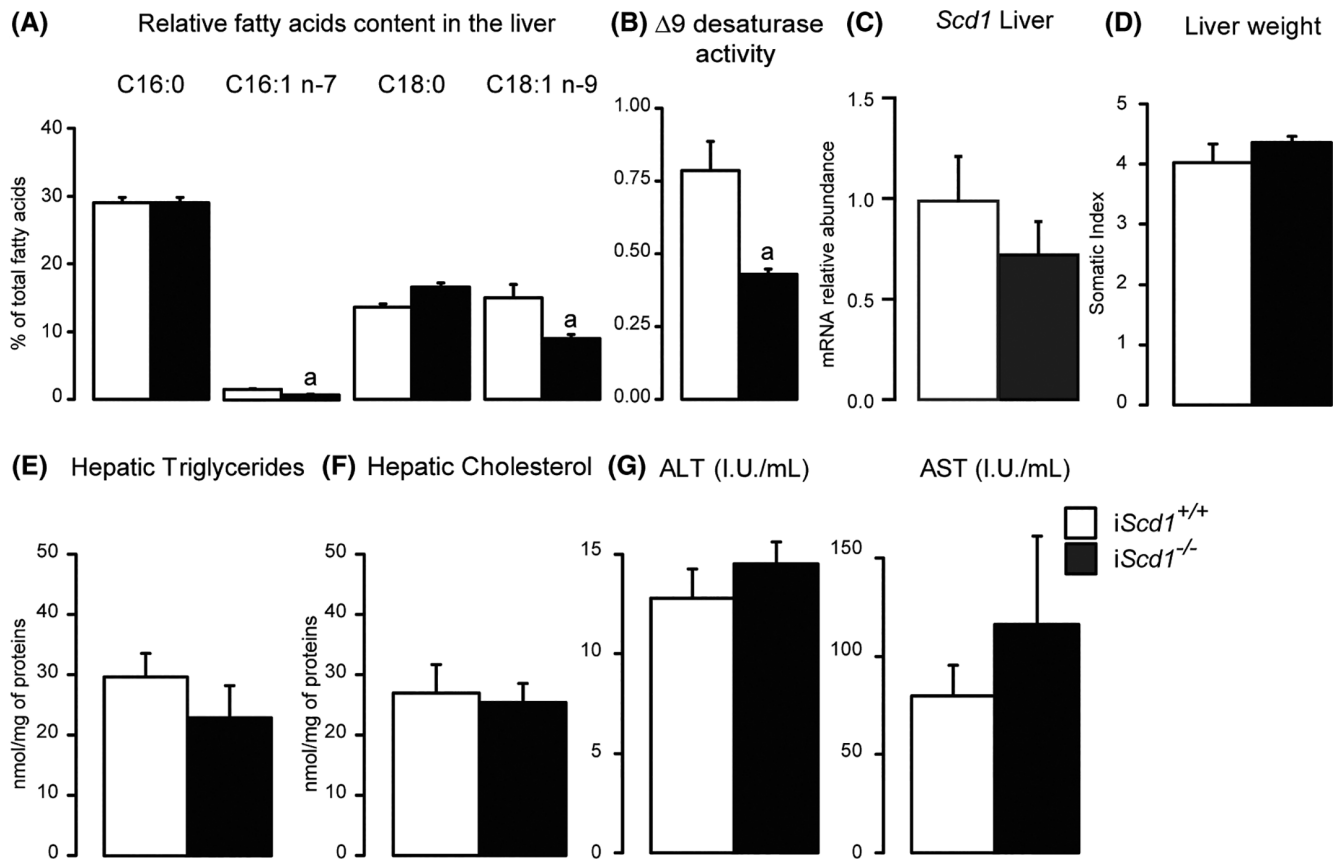

FIGURE 1 Intestinal stearoyl-CoA desaturase 1 (*Scd1*) deletion drives hepatic fatty acids profile dysregulation. (A) Hepatic saturated and mono-unsaturated fatty acids proportions were analyzed by gas chromatography–mass spectrometry of saponified hepatic lipid extracts. (B) Delta-9 desaturase activity is the ratio of mono-unsaturated/saturated fatty acids. Data are presented as the mean of the molar percentage measured in liver of i*Scd1*$^{+/+}$ and i*Scd1*$^{-/-}$ mice. (C) Hepatic *Scd1* messenger RNA (mRNA) levels quantified by quantitative polymerase chain reaction (qPCR) of i*Scd1*$^{+/+}$ and i*Scd1*$^{-/-}$ mice. (D–G) Liver weight (D), liver triglycerides content (E), liver cholesterol content (F), and transaminases (alanine aminotransferase [ALT] and aspartate aminotransferase [AST]) levels (G) were measured in i*Scd1*$^{+/+}$ (n = 5) and i*Scd1*$^{-/-}$ (n = 6) mice. Data are presented as the mean ± SEM. *Significant difference between the two genotypes.

acids. We therefore measured the intestinal expression of *Npc1l1* (Figure 3C) as well as farnesoid X receptor target genes in the intestine (*Fgf15* [fibroblast growth factor 15]) and in the liver (*Shp* [small heterodimer partner]) (Figure 3D), which are proxy for enterohepatic dysregulation of bile acids metabolism. None of these genes displayed an increased expression in i*Scd1*$^{-/-}$ mice (Figure 3C,D), suggesting that intestinal cholesterol absorption is not elevated in i*Scd1*$^{-/-}$ mice. Therefore, we focused on cholesterol excretion. As both intestine and liver are involved in this process, via trans-intestinal cholesterol efflux[25] and biliary[26] pathways, respectively, we measured the expression of genes encoding for cholesterol transporters. In both ileal mucosa and liver, intestinal *Scd1* deletion decreases the expression of ATP-binding cassette g5 (*Abcg5*) and *Abcg8* (Figure 3E,F). These results suggest that cholesterol accumulation in the intestine, in the liver, and in the blood are the consequence of a defect of cholesterol excretion from the body. The major transcriptional player that regulates cholesterol efflux via both biliary and intestinal pathways is the LXR. The increased systemic cholesterol content as well as the reduced expression of *Abcg5* and *Abcg8* in both intestine and liver suggest a lower LXR activity in i*Scd1*$^{-/-}$ mice versus i*Scd1*$^{+/+}$ mice. This hypothesis is strengthened by the hepatic regulation of LXR target genes involved in lipogenesis (acetyl-CoA carboxylase alpha [*Acaca*], fatty acids synthase [*Fasn*], fatty acids elongase 6 [*Elovl6*], and *Scd1*), whose expression is reduced in i*Scd1*$^{-/-}$ mice versus wild-type animals (Figure 3G). Our results are supported by the fact that the whole-body *Scd1*-KO mice fed an oleate-deprived diet displayed a similar regulation of these LXR target genes (Figure S1). Thus, we hypothesized that following dietary oleate deficiency, intestinal *Scd1* deletion would hamper the generation of a circulating LXR-activating signal that would affect both the intestine and the liver. We assayed LXRα and LXRβ activity in HeLa cells with a luciferase reporter assay. Cells were cultured with the plasma of mice from both genotypes fed the OAD diet. Plasma from i*Scd1*$^{-/-}$ mice was less potent to trigger LXRα activity than the one from their wild-type littermates (Figure 3H).

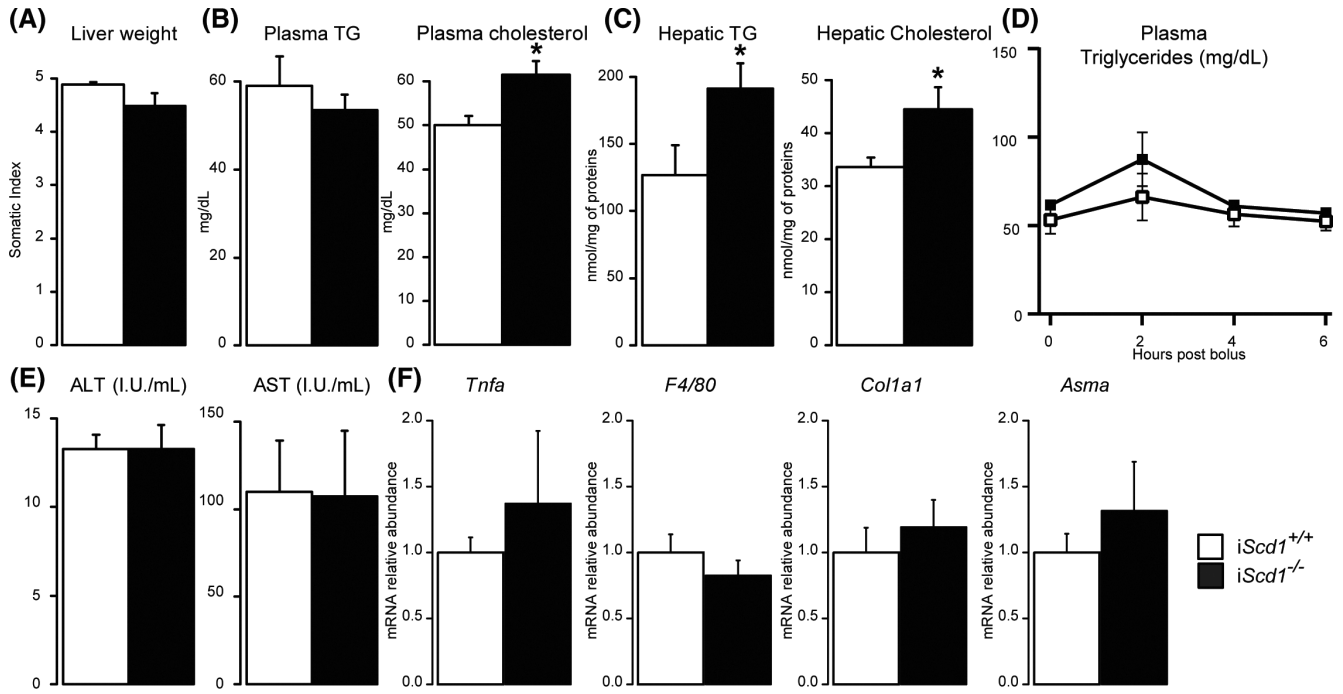

FIGURE 2 Dietary oleate deficiency reveals the role of intestinal *Scd1* in the regulation of hepatic neutral lipids content. (A–D) Liver weight (A), plasma (B), hepatic triglyceride and cholesterol levels (C), and circulating triglycerides (D) after a 200-μL hydrogenated palm oil bolus in fasted i*Scd1*$^{+/+}$ (n = 5) and i*Scd1*$^{-/-}$ (n = 6) mice after 8 weeks of an oleic acid–deficient (OAD) diet feeding. (E) Plasma transaminases (ALT and AST) levels were measured in i*Scd1*$^{+/+}$ (n = 5) and i*Scd1*$^{-/-}$ (n = 6) mice fed an OAD diet during 8 weeks. (F) Hepatic *Tnfa*, *F4/80*, *Col1a1*, and *Asma* mRNA levels quantified by quantitative PCR of i*Scd1*$^{+/+}$ (n = 5) and i*Scd1*$^{-/-}$ (n = 6) mice fed the OAD diet during 8 weeks. Data are presented as the mean ± SEM. *Significant difference between the two genotypes. Asma, alpha smooth muscle actin; Col1a1, collagen 1a1; Tnfα, tumor necrosis factor α.

We observed no differences regarding LXRβ activity (Figure 3H). Collectively, these results suggest a lower intestinal and hepatic cholesterol excretion that could be driven by a lower LXR activity in i*Scd1*$^{-/-}$ mice compared with their wild-type littermates when fed the OAD diet. To confirm the implication of intestinal SCD1 as a key player of general cholesterol metabolism, we fed i*Scd1*$^{+/+}$ and i*Scd1*$^{-/-}$ mice chow and cholesterol enriched (2%) diets during a week. This diet has been shown to induce LXR activity and target genes in both liver and intestine.[27,28] Then, we measured plasma cholesterol (Figure 3I) and observed that i*Scd1*$^{-/-}$ mice display a higher hypercholesterolemia compared with wild-type mice fed with the same cholesterol-rich diet (Figure 3H). This result confirms that i*Scd1*$^{-/-}$ mice are not able to cope with excess cholesterol.

High-fat, high-cholesterol diet triggers inflammation and fibrosis in i*Scd1*$^{-/-}$ mice

To study the hepatic consequences of intestinal *Scd1* deletion on a long-term high-cholesterol dietary supply, we fed i*Scd1*$^{-/-}$ and i*Scd1*$^{+/+}$ mice with chow and high-fat/high-cholesterol Western diets (WD) for 4 months. We followed body weight gain. Although both genotypes display equal food intake, i*Scd1*$^{-/-}$ gained more weight compared with their wild-type littermates when fed with WD (Figure S2A). No difference occurred following chow feeding (Figure 4A). Liver weight was not affected by the genotype in both chow diet and WD feeding (Figure 4A). We also performed an oral glucose tolerance test and observed that intestinal deletion of *Scd1* impaired glucose handling when mice were fed the WD (Figure S2B).

FIGURE 3 Intestinal *Scd1* deletion impacts systemic cholesterol homeostasis. (A) Hepatic *Hmgcr*, *Mvd*, and *Fdps* mRNA levels quantified by quantitative PCR of i*Scd1*$^{+/+}$ (n = 5) and i*Scd1*$^{-/-}$ (n = 6) mice fed OAD diet during 8 weeks. (B) Ileal cholesterol content assayed in mucosal lipid extracts of i*Scd1*$^{+/+}$ (n = 5) and i*Scd1*$^{-/-}$ (n = 6) mice fed the OAD diet during 8 weeks. (C–G) Ileal *Npc1l1* (C), ileal *Fgf15* and hepatic *Shp* (D), ileal *Abcg5* and *Abcg8* (E), hepatic *Abcg5* and *Abcg8* (F), and hepatic *Acaca*, *Fasn*, *Elovl6* and *Scd1* mRNA levels (G) quantified by quantitative PCR of i*Scd1*$^{+/+}$ (n = 5) and i*Scd1*$^{-/-}$ (n = 6) mice fed the OAD diet during 8 weeks. (H) *In vitro* LXR alpha and beta activity assay in response to plasma from i*Scd1*$^{+/+}$ and i*Scd1*$^{-/-}$ mice fed the OAD diet (n = 6 plasma/group). Data are presented as the mean ± SEM. *Significant difference between the two genotypes. (I) Plasma cholesterol levels measured in i*Scd1*$^{+/+}$ and i*Scd1*$^{-/-}$ mice fed chow or cholesterol-enriched (2% cholesterol) chow diets during 1 week (n = 6 mice /group). [a]Significant difference between the two genotypes for a given diet. [b]Significant difference between the two genotypes for a given genotype. Abcg5, ATP-binding cassette g5; Abcg8, ATP-binding cassette g8; Acaca, acetyl-CoA carboxylase alpha; Elovl6, fatty acids elongase 6; Fasn, fatty acids synthase; Fdps, farnesyl diphosphate synthase; Fgf15, fibroblast growth factor 15; Hmgcr, 3-hydroxy 3-methylglutaryl-CoA reductase; Lxr, liver X receptor; Mvd, mevalonate diphosphate decarboxylase; Npc1l1, NPC1 like intracellular cholesterol transporter 1; Shp, small heterodimer partner.

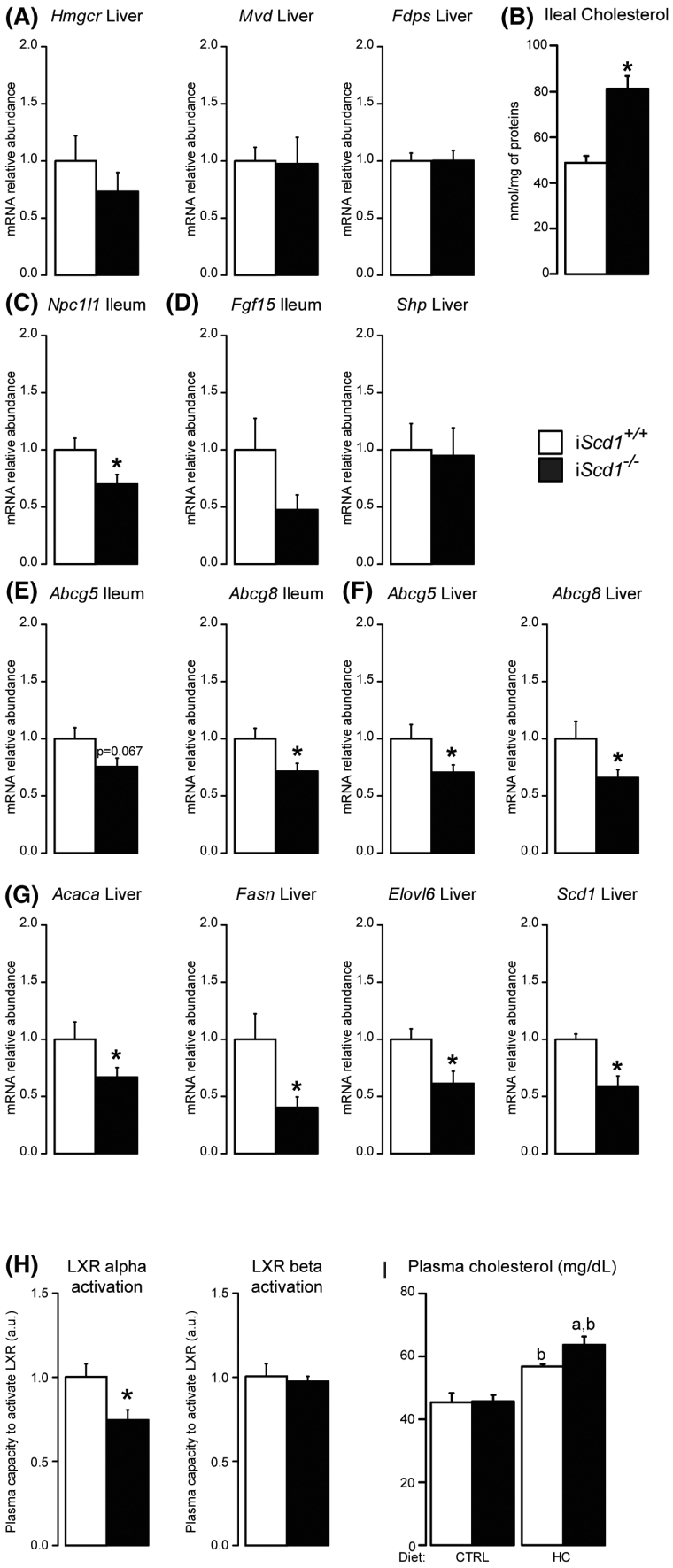
(A) Hmgcr Liver
Mvd Liver
Fdps Liver
(B) Ileal Cholesterol
mRNA relative abundance
nmol/mg of proteins
(C) Npc1l1 Ileum
(D) Fgf15 Ileum
Shp Liver
iScd1+/+
iScd1-/-
(E) Abcg5 Ileum
Abcg8 Ileum
(F) Abcg5 Liver
Abcg8 Liver
p=0.067
(G) Acaca Liver
Fasn Liver
Elovl6 Liver
Scd1 Liver
(H) LXR alpha activation
LXR beta activation
Plasma cholesterol (mg/dL)
Plasma capacity to activate LXR (a.u.)
a,b
b
Diet:
CTRL
HC

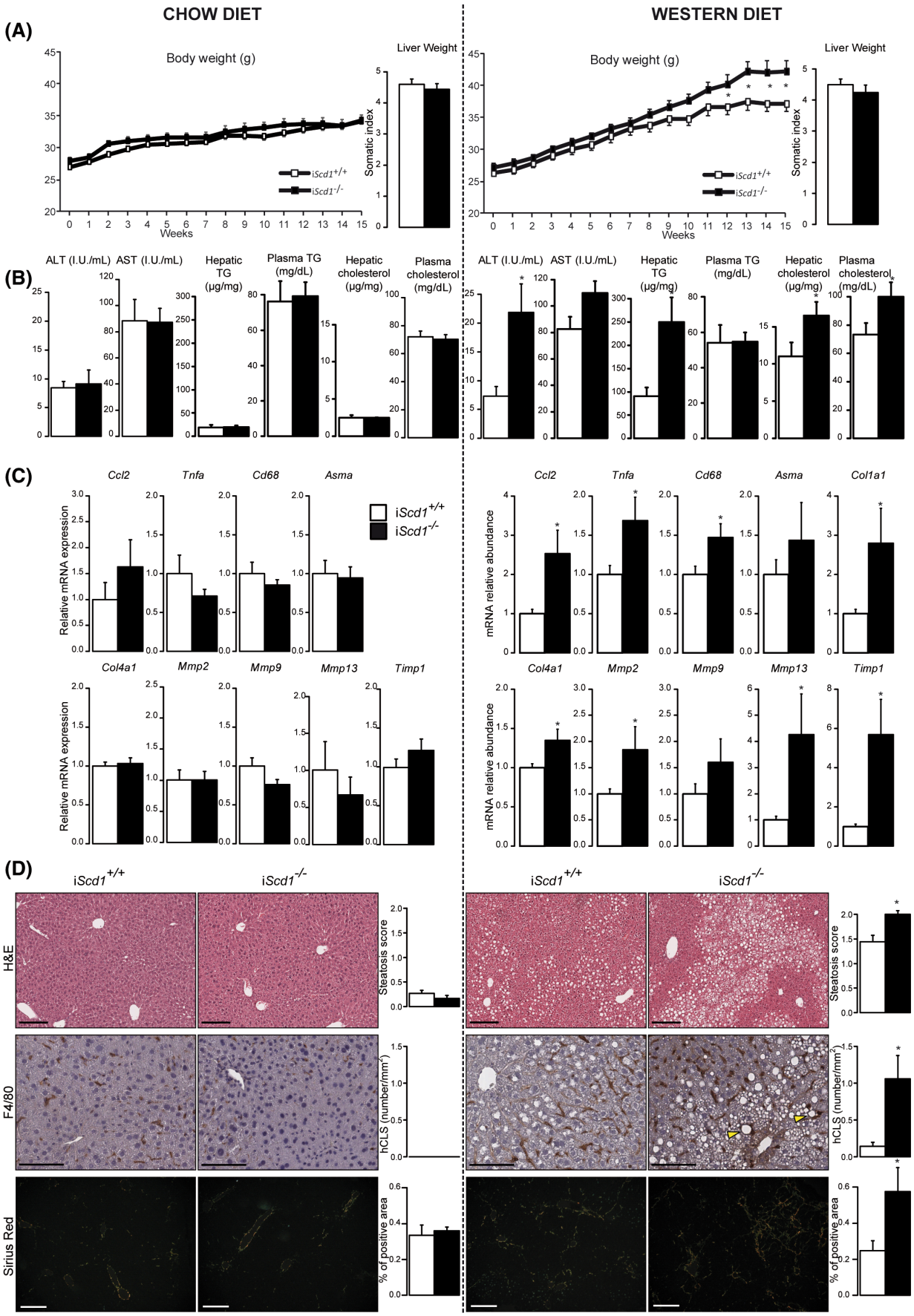
CHOW DIET
WESTERN DIET
(A)
Body weight (g)
Weeks
Liver Weight
Somatic index
iScd1+/+
iScd1-/-
(B)
ALT (I.U./mL)
AST (I.U./mL)
Hepatic TG (µg/mg)
Plasma TG (mg/dL)
Hepatic cholesterol (µg/mg)
Plasma cholesterol (mg/dL)
(C)
Ccl2
Tnfa
Cd68
Asma
Col1a1
Col4a1
Mmp2
Mmp9
Mmp13
Timp1
Relative mRNA expression
mRNA relative abundance
(D)
H&E
F4/80
Sirius Red
Steatosis score
hCLS (number/mm2)
% of positive area

FIGURE 4 High-fat high-cholesterol diet triggers nonalcoholic steatohepatitis in i*Scd1*$^{-/-}$ mice. (A) Body weight evolution and liver weight at sacrifice of i*Scd1*$^{+/+}$ and i*Scd1*$^{-/-}$ mice fed chow (n = 6 animals/group) or Western diet (n = 9 animals/group) for 16 weeks. (B) Plasma ALT, AST, and cholesterol levels quantified by colorimetric test of i*Scd1*$^{+/+}$ and i*Scd1*$^{-/-}$ mice fed chow (n = 6 animals/group) or Western diet (n = 9 animals/group). Hepatic cholesterol and triglycerides quantified by gas chromatography coupled with an FID detector of i*Scd1*$^{+/+}$ and i*Scd1*$^{-/-}$ mice fed chow (n = 6 animals/group) or Western diet (n = 9 animals/group). (C) Hepatic *Ccl2*, *Tnfa*, *Cd68*, *Asma*, *Col1a1*, *Col4a1*, *Mmp2*, *Mmp9*, *Mmp13*, and *Timp1* mRNA levels quantified by quantitative PCR of i*Scd1*$^{+/+}$ and i*Scd1*$^{-/-}$ mice fed chow (n = 6 animals/group) or Western diet (n = 9 animals/group). (D) Representative hematoxylin and eosin (H&E; scale bar: 200 μm), F4/80 (scale bar: 100μm), and sirius red (scale bar: 200 μm) staining sections of liver and respective quantification of steatosis, hepatic crown like structure (hCLS, highlighted with yellow arrow), and sirius red positive area from mice of both genotypes fed chow (n = 6 animals/group) or Western diet (n = 9 animals/group). Data are presented as the mean ± SEM. *Significant difference between the two genotypes. Ccl2, chemokine ligand 2; Col1a1, collagen 1a1; Col4a1, collagen 4a1; Mmp, matrix metallopeptidase 2; Timp1, metallopeptidase inhibitor.

We next measured plasma content of transaminases and cholesterol, and hepatic levels of cholesterol and triglycerides (Figure 4B). Intestinal deletion of *Scd1* results in significantly elevated ALT, plasma cholesterol, liver cholesterol, and liver TG levels, and tended to increase AST in WD fed mice. Hepatic neutral lipids accumulation was histologically confirmed by H&E staining and steatosis scoring (Figure 4D). In mice fed with the chow diet, no difference was observed between the two genotypes (Figure 4B,D). As hepatic neutral lipids were affected by intestinal *Scd1* deletion, we also determined hepatic FA profile. Strikingly, in WD-fed mice, oleate levels were elevated and palmitoleate proportion tended to be increased in i*Scd1*$^{-/-}$ versus i*Scd1*$^{+/+}$ mice (Figure S2C). These modulations are concomitant to a trend toward the overexpression of *Scd1* in the liver (Figure S2D). It is interesting to note that, in contrast, the expression of *Acaca* and *Fasn*, two other LXR target genes involved in *de novo* lipogenesis, are decreased in i*Scd1*$^{-/-}$ versus i*Scd1*$^{+/+}$ mice (Figure S2E). To further explore the potent hepatic dysfunction highlighted by the elevation of ALT and hepatic cholesterol levels, we next measured the expression of gene markers of inflammation (chemokine ligand 2 [*Ccl2*], *Tnfa*, and *Cd68*) and fibrosis (*Asma*, *Col1a1*, *Col4a1*, matrix metallopeptidase 2 [*Mmp2*], *Mmp9*, *Mmp13*, and metallopeptidase inhibitor [*Timp1*]) (Figure 4C). Hepatic levels of *Ccl2*, *Tnfa*, *Cd68*, *Col1a1*, *Col4a1*, *Mmp2*, *Mmp13*, and *Timp1* were more elevated in i*Scd1*$^{-/-}$ mice than in their wild-type littermates both under WD. Again, no difference was observed between mice of both genotype fed the chow diet (Figure 4C). To confirm the inflammatory and fibrotic phenotype in livers of i*Scd1*$^{-/-}$ mice fed the WD, we counted hepatic crown-like structure (hCLS) after F4/80 immunohistochemical staining and evaluated collagen fibers deposition with sirius red (Figure 4D). When challenged with the WD, i*Scd1*$^{-/-}$ mice displayed higher hCLS number and hepatic collagen deposition compared with i*Scd1*$^{+/+}$ mice (Figure 4D). No changes in hCLS were detectable following chow diet feeding, whatever the genotype. Intestinal *Scd1* deletion did not affect collagen deposition in the liver when mice were fed the chow diet. However, these data suggest that intestinal SCD1 protects from inflammation and fibrosis induced by high-fat and high-cholesterol diet.

Intestinal deletion of *Scd1* favors cancer progression in a chemical model of HCC

Cholesterol in NASH[29] is one of the factors that predisposes to HCC onset. Because intestinal *Scd1* deletion triggers dysregulation of cholesterol metabolism together with inflammation and fibrosis, we hypothesized that i*Scd1*$^{-/-}$ mice would be more prone to cancer development compared with their wild-type littermates. This hypothesis was strengthened by the fact that total-body SCD1-KO mice fed a fat-free diet displayed high hepatic cholesterol content and mRNA cancer markers such as cyclin-dependent kinase 1 (*Cdk1*), Myc proto-oncogene (*Myc*), Src proto-oncogene (*Src*), Marker of proliferation Ki67 (*Ki67*), Adam metallopeptidase 10 (*Adam10*), and phosphate and tensin homolog (*Pten*) (Figure S3A). Even if at the steady state there is trend—although not significant—in the difference of cyclin D1 (*Ccnd1*) and cyclin E1 (*Ccne1*) expression (Figure S3B) between the genotypes, one cannot exclude that the absence of intestinal *Scd1* could drive the proliferation capacity of the hepatocytes under specific regenerative stimulus. To test this hypothesis, we injected 14-day-old pups of both genotype with diethylnitrosamine, a chemical carcinogen able to induce liver tumor. We did not add extra stimuli like dietary deprivation of oleic acid or cholesterol supply. The hepatic MUFA profile is already altered in i*Scd1*$^{-/-}$ mice fed the chow diet (Figure 1A), so this modulation would be sufficient to predispose to cancer progression, given the long duration of HCC progression in this model. At 1 year old, body and liver weights were respectively decreased and increased in i*Scd1*$^{-/-}$ mice compared with their wild-type littermates (Figure 5A,B). Lower body weight and higher liver weight are markers of cancer progression. Although we did not observe difference in tumor number between the two genotypes (Figure 5C), i*Scd1*$^{-/-}$ mice showed an increased tumor progression (Figure 5D), bigger tumors (Figure 5E), and more metastasis in the lungs (Figure 5F) compared with their wild-type littermates. However, we did not observe any modulation of proliferation genes (*Ccnd1*, *Ccne1*, and *Myc*) in tumors or adjacent tissue (Figure S3C,D). Collectively, these data suggest that the disturbances of the hepatic FA profile induced by intestinal *Scd1*

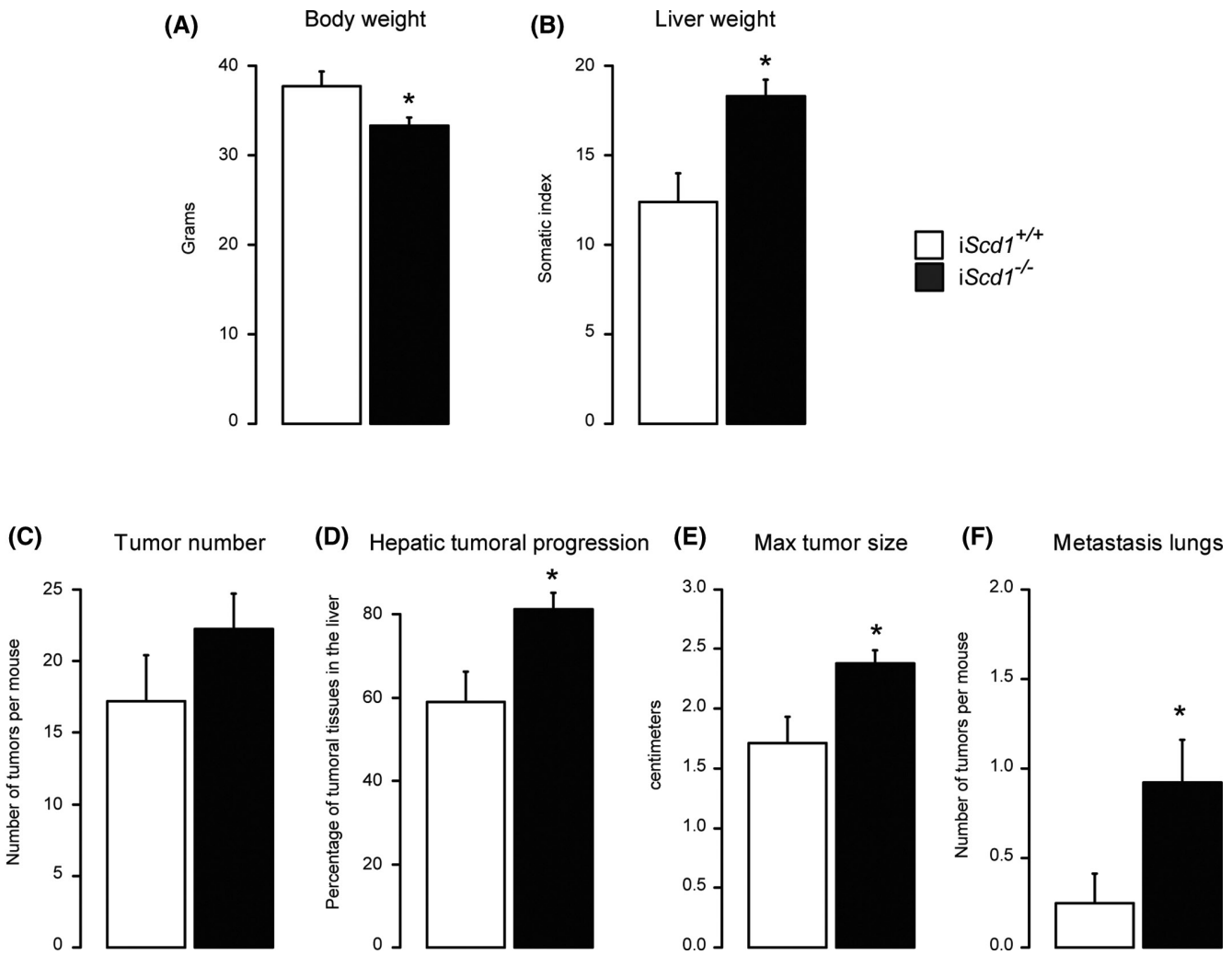

FIGURE 5 Intestinal deletion of Scd1 favors tumor progression in a chemically induced model of hepatocellular carcinoma. (A,B) Body (A) and liver (B) weight of i*Scd1*$^{+/+}$ (n = 9) and i*Scd1*$^{-/-}$ (n = 13) male mice injected with diethylnitrosamine. (C–F) Number of hepatic tumors (C), percentage of tumor tissue in the liver (D), size of the biggest hepatic tumor (E), and member of lung metastasis (F) of i*Scd1*$^{+/+}$ (n = 9) and i*Scd1*$^{-/-}$ (n = 13) male mice injected with diethylnitrosamine (n = 9–13 animals/group). Data are presented as the mean ± SEM. *Significant difference between the two genotypes.

deletion are sufficient to favor tumor progression in a DEN-induced HCC model, despite no dietary deprivation of oleic acid and no supply of cholesterol.

DISCUSSION

FAs play a major role in hepatic metabolic functions. Indeed, it has been shown that all FA families (n-6, n-3, and mono-unsaturated and saturated FAs) control numerous aspects of hepatic homeostasis,[30] like lipogenesis[23] and FA oxidation.[31] It has already been shown that MUFAs displayed beneficial effects in liver: their accumulation during steatosis is dissociated from inflammation or insulin resistance.[32,33] Moreover, in a NASH model induced by dietary choline/methionine deficiency, *Scd1* deletion in the whole organism favored hepatic damages despite a reduced steatosis.[8] Patients with NASH are characterized by altered hepatic and circulating MUFA species that significantly correlate with the progression of the disease.[34] Collectively, these data highlight the important roles of MUFAs in preserving hepatic functions. Hepatic MUFAs derive by several pathways, including adipose tissue lipolysis, hepatic lipogenesis, and intestinal absorption of dietary supplies.[4] The intestinal source is of peculiar importance, especially given the increasing prevalence of obesity and obesity-related diseases that are driven primarily by a modulation of quantity and quality of ingested food. Indeed, the intestine plays a major role in controlling nutrients intake, via notably regulating lipid absorption, modification, trafficking, and excretion. Although the intestine is not considered as a lipogenic organ *per se*, in the enterocytes, dietary-derived free FAs are elongated, desaturated, and esterified to form triglycerides, phospholipids, and cholesterol esters. Only few studies have documented the role of intestinal lipogenesis in the intestine itself. *De novo* lipogenesis

is of importance in maintaining some of its functions including intestinal permeability.[15] Indeed, intestinal deletion of the FA synthase leads to a disruption in intestinal mucus layer, an increase of intestinal permeability and inflammation.[15] However, extra-intestinal consequences of the gut lipogenesis and FA handling have not been explored yet.

We previously showed that intestinal *Scd1* deletion drives intestinal inflammation and tumorigenesis. Here, we wanted to explore the extra-intestinal effects of *Scd1* deletion in the gut, focusing primarily on the liver, as this organ is tightly connected to the intestine. We first showed that intestinal *Scd1* deletion decreased hepatic MUFA levels (Figure 1A) without compensation of hepatic *Scd1* expression (Figure 1C), suggesting, at basal state, a direct contribution of gut-derived MUFAs on hepatic MUFA content. We then challenged these mice with an oleic acid–deprived diet, and lipid analysis revealed an increased hepatic content of TGs and cholesterol without apparent signs of hepatic damage compared with their wild-type littermates (Figure 2). Following acute TG bolus challenge, i*Scd1*$^{-/-}$ mice tend to absorb more TG than i*Scd1*$^{+/+}$ mice (Figure 2D). This could contribute to the hepatic TG accumulation during to the chronic exposition of animals to OAD (Figure 2C) or WD (Figure 4B). When fed an OAD, global *Scd1* KO mice display hypercholesterolemia and hepatic cholesterol accumulation.[21,22] As cholesterol is a major driver of NAFLD progression, we focused on this molecule. Our transcriptomic data suggest that systemic cholesterol dysregulation observed in i*Scd1*$^{-/-}$ mice fed the OAD diet could be a consequence of a defect of trans-intestinal and biliary cholesterol excretion linked with a defect of LXR activation (Figure 3). We therefore studied the long-term effects of a cholesterol-rich diet and fed mice a WD containing 0.2% cholesterol for 4 months. Compared with their wild-type littermates, i*Scd1*$^{-/-}$ mice developed hepatic inflammation and fibrosis associated with hepatic cholesterol accumulation and hypercholesterolemia (Figure 4). Here, inflammation and fibrosis occurred concomitantly with an increase of hepatic oleate proportion and a trend toward hepatic *Scd1* overexpression (Figure S2C,D) that can be interpreted as an attempt to provide liver with MUFAs when gut MUFA production is deleted. However, literature suggests that this could be a protective mechanism[32,33]; the origin and the precise role of hepatic MUFA accumulation in this model requires further investigation.

SCD1 has already been linked with cholesterol. When fed a high-carbohydrate low-fat (and therefore low in MUFA) diet, total body *Scd1*-KO mice developed hypercholesterolemia (more than a 100% increase, depending the sex) and hepatic cholesterol accumulation,[21,22] although hepatocyte-specific *Scd1*-KO mice display only a 50% increase of cholesterolemia when fed the same diet.[10] This difference suggests that extrahepatic SCD1 activity could contribute to modulate cholesterolemia. The role of cholesterol in NASH development has been documented extensively (reviewed in Ioannou[29]). Cholesterol accumulation in the liver disturbs hepatocyte homeostasis as well as Kupffer cells[35] and hepatic stellate cells,[36] whose activation triggers inflammation and fibrosis, respectively. Intestinal deletion of *Scd1* triggered hypercholesterolemia in mice fed the OAD and the cholesterol-rich diets. In OAD-fed and WD-fed KO animals, we also observed hepatic cholesterol accumulation (Figures 2C and 4B). The concomitant dysregulation of cholesterol homeostasis in our model could be the hit triggering inflammation and fibrosis in i*Scd1*$^{-/-}$ mice fed the high-fat high-cholesterol WD (Figure 4). In this study, we showed that intestinal *Scd1* deletion was decreasing LXR transcriptional activity in both the intestine and the liver in different NAFLD models (Figures 2–4). In the literature, LXR activity up-regulation by MUFAs has been already suggested in liver[37] and neutrophils.[38] Here, without providing a formal demonstration that LXR activity is increased by SCD1 enzymatic function, we highlight a strong link that suggests such a regulation. Moreover, despite an accumulation of cholesterol (Figures 2C and 3B) and potentially of oxysterols, the induction of LXR transcriptional activity appears to require intestinal SCD1 and *de novo* MUFA generation.

Finally, we also focused on the implication of the intestinal *Scd1* deletion on HCC development. It is well recognized that NASH predisposes to HCC: after hepatitis C virus infection and alcohol-associated liver diseases, it is the third most common cause of HCC and its importance is rising in the United States.[39] Hepatic FA profile is deeply modulated in mice[40] and patients[41] displaying HCC. Specifically, MUFA species proportion increases with HCC[40,41]; however, whether this dysregulation is a hit triggering HCC or is a compensatory mechanism potentially rescuing the phenotype has not yet been defined. As the intestinal *Scd1* deletion without particularly regimen was sufficient to decrease hepatic MUFA proportion (Figure 1A), we injected both wild-type and KO chow-fed mice with DEN, a carcinogen triggering hepatic damage and leading to hepatic cancer lesions. After 1 year, i*Scd1*$^{-/-}$ mice displayed higher HCC progression, bigger tumors, and more metastasis in the lungs compared with their wild-type littermates (Figure 5). However, we did not observe modulation of genes involved in cellular proliferation between genotypes in both tumors and adjacent tissue (Figure S3C,D). In our opinion, the cancerous lesions are too advanced to draw any conclusions about a potential mechanism leading to the more severe phenotype observed in i*Scd1*$^{-/-}$ mice. These data suggest that intestinal-derived MUFAs are sufficient to affect hepatic FA profile and to sensitize the liver to cancer progression. This result spread the light of the importance of gut-derived, and thus dietary MUFA supply, in

the prevention of HCC. Adherence to the Mediterranean diet, of which olive oil and thus oleic acid is a universal component, has been shown to decrease cancer incidence (reviewed in Lopez-Miranda et al.[42]). Although its effect has not been described specifically on HCC, the effect of MUFA-rich diet toward HCC development is worth testing in several animal models.

Collectively, these results highlight that the intestine-derived MUFAs are of importance in the whole-body lipid homeostasis. Specifically, delta-9 desaturation impairment in this organ leads to systemic and hepatic dysregulation of FA and cholesterol metabolism with increased susceptibility to severe liver diseases like NASH and HCC.

All authors had access to the study data and reviewed and approved the final manuscript.

AUTHOR CONTRIBUTIONS

Study design: Simon Ducheix, Carlo Sabbà, and Antonio Moschetta. *Data analysis*: Simon Ducheix, Carlo Sabbà, and James M. Ntambi. *Experiments and statistical analysis*: Simon Ducheix. *Manuscript draft*: Simon Ducheix and Antonio Moschetta. *Gene expression and mouse studies*: Elena Piccinin and Oihane Garcia-Irigoyen. *Histology*: Claudia Peres and Marica Cariello. In vitro *LXR activity experiments*: Allan Fouache and Jean-Marc Lobaccaro. *Lipidomic measurements and analysis*: Hervé Guillou. *Scd expertise and data comments*: James M. Ntambi. *Study supervision*: Antonio Moschetta.

ACKNOWLEDGMENT

The authors thank the members of the Metatoul Facility for the fatty acids profile. MetaToul (Toulouse metabolomics & fluxomics facilities, www.metatoul.fr) is part of the French National Infrastructure for Metabolomics and Fluxomics MetaboHUB-ANR-11-INBS-0010. They also thank Michele Minuto, Angelo Quaranta, and members of the laboratory for their help during the mouse studies.

FUNDING INFORMATION

Supported by the Italian Association for Cancer Research (AIRC IG 2019 Id 23239); EU-JPI HDL-INTIMIC MIUR - FATMAL 2017; MIUR-PRIN 2017 Cod. 2017 J3E2W2; MIUR-PON “R&I” 2014–2020 “BIOMIS” Cod. ARS01_01220; POR Puglia FESR - FSE 2014–2020 “INNOMA” Cod. 4TCJLV4; and Attività 2, linea 1 (PON AIM1853334).

CONFLICT OF INTEREST

Nothing to report.

ETHICS STATEMENT

The Ethical Committee of the University of Bari approved this experimental setup, which also was certified by the Italian Ministry of Health in accordance with internationally accepted guidelines for animal care.

ORCID

Simon Ducheix https://orcid.org/0000-0001-6676-4263
Elena Piccinin https://orcid.org/0000-0002-6514-2689
Jean-Marc Lobaccaro https://orcid.org/0000-0001-9890-2392

REFERENCES

1. Marchesini G, Marzocchi R, Agostini F, Bugianesi E. Nonalcoholic fatty liver disease and the metabolic syndrome. Curr Opin Lipidol. 2005;16:421–7.
2. Marchesini G, Brizi M, Morselli-Labate AM, Bianchi G, Bugianesi E, McCullough AJ, et al. Association of nonalcoholic fatty liver disease with insulin resistance. Am J Med. 1999;107:450–5.
3. Tilg H, Moschen AR. Evolution of inflammation in nonalcoholic fatty liver disease: the multiple parallel hits hypothesis. Hepatology. 2010;52:1836–46.
4. Donnelly KL, Smith CI, Schwarzenberg SJ, Jessurun J, Boldt MD, Parks EJ. Sources of fatty acids stored in liver and secreted via lipoproteins in patients with nonalcoholic fatty liver disease. J Clin Invest. 2005;115:1343–51.
5. Ntambi JM, Miyazaki M, Stoehr JP, Lan H, Kendziorski CM, Yandell BS, et al. Loss of stearoyl-CoA desaturase-1 function protects mice against adiposity. Proc Natl Acad Sci U S A. 2002;99:11482–6.
6. Cohen P, Miyazaki M, Socci ND, Hagge-Greenberg A, Liedtke W, Soukas AA, et al. Role for stearoyl-CoA desaturase-1 in leptin-mediated weight loss. Science. 2002;297:240–3.
7. MacDonald ML, van Eck M, Hildebrand RB, Wong BW, Bissada N, Ruddle P, et al. Despite antiatherogenic metabolic characteristics, SCD1-deficient mice have increased inflammation and atherosclerosis. Arterioscler Thromb Vasc Biol. 2009;29:341–7.
8. Li ZZ, Berk M, McIntyre TM, Feldstein AE. Hepatic lipid partitioning and liver damage in nonalcoholic fatty liver disease: role of stearoyl-CoA desaturase. J Biol Chem. 2009;284:5637–44.
9. Binczek E, Jenke B, Holz B, Gunter RH, Thevis M, Stoffel W. Obesity resistance of the stearoyl-CoA desaturase-deficient (scd1-/-) mouse results from disruption of the epidermal lipid barrier and adaptive thermoregulation. Biol Chem. 2007;388:405–18.
10. Miyazaki M, Flowers MT, Sampath H, Chu K, Otzelberger C, Liu X, et al. Hepatic stearoyl-CoA desaturase-1 deficiency protects mice from carbohydrate-induced adiposity and hepatic steatosis. Cell Metab. 2007;6:484–96.
11. Burhans MS, Flowers MT, Harrington KR, Bond LM, Guo CA, Anderson RM, et al. Hepatic oleate regulates adipose tissue lipogenesis and fatty acid oxidation. J Lipid Res. 2015;56:304–18.
12. Marra F, Svegliati-Baroni G. Lipotoxicity and the gut-liver axis in NASH pathogenesis. J Hepatol. 2018;68:280–95.
13. De Vadder F, Kovatcheva-Datchary P, Zitoun C, Duchampt A, Backhed F, Mithieux G. Microbiota-produced succinate improves glucose homeostasis via intestinal gluconeogenesis. Cell Metab. 2016;24:151–7.
14. Kim M, Astapova II, Flier SN, Hannou SA, Doridot L, Sargsyan A, et al. Intestinal, but not hepatic, ChREBP is required for fructose tolerance. JCI Insight. 2017;2:e96703.
15. Wei X, Yang Z, Rey FE, Ridaura VK, Davidson NO, Gordon JI, et al. Fatty acid synthase modulates intestinal barrier function through palmitoylation of mucin 2. Cell Host Microbe. 2012;11:140–52.
16. Ducheix S, Peres C, Hardfeldt J, Frau C, Mocciaro G, Piccinin E, et al. Deletion of stearoyl-CoA desaturase-1 from the intestinal

epithelium promotes inflammation and tumorigenesis, reversed by dietary oleate. Gastroenterology. 2018;155:1524–38.e1529.
17. Kleiner DE, Brunt EM, Van Natta M, Behling C, Contos MJ, Cummings OW, et al. Design and validation of a histological scoring system for nonalcoholic fatty liver disease. Hepatology. 2005;41:1313–21.
18. Fouache A, Zabaiou N, De Joussineau C, Morel L, Silvente-Poirot S, Namsi A, et al. Flavonoids differentially modulate liver X receptors activity-Structure-function relationship analysis. J Steroid Biochem Mol Biol. 2019;190:173–82.
19. Sekiya M, Yahagi N, Matsuzaka T, Najima Y, Nakakuki M, Nagai R, et al. Polyunsaturated fatty acids ameliorate hepatic steatosis in obese mice by SREBP-1 suppression. Hepatology. 2003;38:1529–39.
20. Ioannou GN, Subramanian S, Chait A, Haigh WG, Yeh MM, Farrell GC, et al. Cholesterol crystallization within hepatocyte lipid droplets and its role in murine NASH. J Lipid Res. 2017;58:1067–79.
21. Flowers MT, Groen AK, Oler AT, Keller MP, Choi Y, Schueler KL, et al. Cholestasis and hypercholesterolemia in SCD1-deficient mice fed a low-fat, high-carbohydrate diet. J Lipid Res. 2006;47:2668–80.
22. Flowers MT, Keller MP, Choi Y, Lan H, Kendziorski C, Ntambi JM, et al. Liver gene expression analysis reveals endoplasmic reticulum stress and metabolic dysfunction in SCD1-deficient mice fed a very low-fat diet. Physiol Genomics. 2008;33:361–72.
23. Ducheix S, Montagner A, Polizzi A, Lasserre F, Marmugi A, Bertrand-Michel J, et al. Essential fatty acids deficiency promotes lipogenic gene expression and hepatic steatosis through the liver X receptor. J Hepatol. 2013;58:984–92.
24. Bovenga F, Sabba C, Moschetta A. Uncoupling nuclear receptor LXR and cholesterol metabolism in cancer. Cell Metab. 2015;21:517–26.
25. van der Veen JN, van Dijk TH, Vrins CL, van Meer H, Havinga R, Bijsterveld K, et al. Activation of the liver X receptor stimulates trans-intestinal excretion of plasma cholesterol. J Biol Chem. 2009;284:19211–9.
26. Zhang Y, Breevoort SR, Angdisen J, Fu M, Schmidt DR, Holmstrom SR, et al. Liver LXRalpha expression is crucial for whole body cholesterol homeostasis and reverse cholesterol transport in mice. J Clin Invest. 2012;122:1688–99.
27. Peet DJ, Turley SD, Ma W, Janowski BA, Lobaccaro JM, Hammer RE, et al. Cholesterol and bile acid metabolism are impaired in mice lacking the nuclear oxysterol receptor LXR alpha. Cell. 1998;93:693–704.
28. Repa JJ, Berge KE, Pomajzl C, Richardson JA, Hobbs H, Mangelsdorf DJ. Regulation of ATP-binding cassette sterol transporters ABCG5 and ABCG8 by the liver X receptors alpha and beta. J Biol Chem. 2002;277:18793–800.
29. Ioannou GN. The Role of Cholesterol in the Pathogenesis of NASH. Trends Endocrinol Metab. 2016;27:84–95.
30. Nagao K, Yanagita T. Bioactive lipids in metabolic syndrome. Prog Lipid Res. 2008;47:127–46.
31. Martin PG, Guillou H, Lasserre F, Dejean S, Lan A, Pascussi JM, et al. Novel aspects of PPARalpha-mediated regulation of lipid and xenobiotic metabolism revealed through a nutrigenomic study. Hepatology. 2007;45:767–77.
32. Benhamed F, Denechaud PD, Lemoine M, Robichon C, Moldes M, Bertrand-Michel J, et al. The lipogenic transcription factor ChREBP dissociates hepatic steatosis from insulin resistance in mice and humans. J Clin Invest. 2012;122:2176–94.
33. Bricambert J, Alves-Guerra MC, Esteves P, Prip-Buus C, Bertrand-Michel J, Guillou H, et al. The histone demethylase Phf2 acts as a molecular checkpoint to prevent NAFLD progression during obesity. Nat Commun. 2018;9:2092.
34. Yamada K, Mizukoshi E, Seike T, Horii R, Terashima T, Iida N, et al. Serum C16:1n7/C16:0 ratio as a diagnostic marker for non-alcoholic steatohepatitis. J Gastroenterol Hepatol. 2019;34:1829–35.
35. Matsuoka M, Tsukamoto H. Stimulation of hepatic lipocyte collagen production by Kupffer cell-derived transforming growth factor beta: implication for a pathogenetic role in alcoholic liver fibrogenesis. Hepatology. 1990;11:599–605.
36. Tosello-Trampont AC, Landes SG, Nguyen V, Novobrantseva TI, Hahn YS. Kuppfer cells trigger nonalcoholic steatohepatitis development in diet-induced mouse model through tumor necrosis factor-alpha production. J Biol Chem. 2012;287:40161–72.
37. Ducheix S, Montagner A, Polizzi A, Lasserre F, Regnier M, Marmugi A, et al. Dietary oleic acid regulates hepatic lipogenesis through a liver X receptor-dependent signaling. PLoS One. 2017;12:e0181393.
38. Reyes-Quiroz ME, Alba G, Saenz J, Santa-Maria C, Geniz I, Jimenez J, et al. Oleic acid modulates mRNA expression of liver X receptor (LXR) and its target genes ABCA1 and SREBP1c in human neutrophils. Eur J Nutr. 2014;53:1707–17.
39. Beste LA, Leipertz SL, Green PK, Dominitz JA, Ross D, Ioannou GN. Trends in burden of cirrhosis and hepatocellular carcinoma by underlying liver disease in US veterans, 2001–2013. Gastroenterology. 2015;149:1471–82.e1475; quiz e1417–1478.
40. Muir K, Hazim A, He Y, Peyressatre M, Kim DY, Song X, et al. Proteomic and lipidomic signatures of lipid metabolism in NASH-associated hepatocellular carcinoma. Cancer Res. 2013;73:4722–31.
41. Yamada K, Mizukoshi E, Sunagozaka H, Arai K, Yamashita T, Takeshita Y, et al. Characteristics of hepatic fatty acid compositions in patients with nonalcoholic steatohepatitis. Liver Int. 2015;35:582–90.
42. Lopez-Miranda J, Perez-Jimenez F, Ros E, De Caterina R, Badimon L, Covas MI, et al. Olive oil and health: summary of the II international conference on olive oil and health consensus report, Jaen and Cordoba (Spain) 2008. Nutr Metab Cardiovasc Dis. 2010;20:284–94.

SUPPORTING INFORMATION

Additional supporting information can be found online in the Supporting Information section at the end of this article.

How to cite this article: Ducheix S, Piccinin E, Peres C, Garcia-Irigoyen O, Bertrand-Michel J, Fouache A, Reduction in gut-derived MUFAs via intestinal stearoyl-CoA desaturase 1 deletion drives susceptibility to NAFLD and hepatocarcinoma. Hepatol Commun. 2022;6:2937–2949. https://doi.org/10.1002/hep4.2053